Journal of Food Protection, Vol. 73, No. 12, 2010, Pages 2256–2262

Active Systems Based on Silver-Montmorillonite Nanoparticles Embedded into Bio-Based Polymer Matrices for Packaging Applications

A. L. INCORONATO,[1] G. G. BUONOCORE,[2] A. CONTE,[1,3] M. LAVORGNA,[2] AND M. A. DEL NOBILE[1,3]*

[1]*Department of Food Science, University of Foggia, Via Napoli, 25-71100 Foggia, Italy;* [2]*Institute of Composite and Biomedical Materials, National Research Council, P. le Enrico Fermi, 1, 80055 Portici, Naples, Italy; and* [3]*Istituto per la Ricerca e le Applicazioni Biotecnologiche per la Sicurezza e la Valorizzazione dei Prodotti Tipici e di Qualità, BIOAGROMED, Via Napoli, 52-71100 Foggia, Italy*

MS 10-095: Received 8 March 2010/Accepted 13 June 2010

ABSTRACT

Silver-montmorillonite (Ag-MMT) antimicrobial nanoparticles were obtained by allowing silver ions from nitrate solutions to replace the Na^+ of natural montmorillonite and to be reduced by thermal treatment. The Ag-MMT nanoparticles were embedded in agar, zein, and poly(ε-caprolactone) polymer matrices. These nanocomposites were tested in vitro with a three-strain cocktail of *Pseudomonas* spp. to assess antimicrobial effectiveness. The results indicate that Ag-MMT nanoparticles embedded into agar may have antimicrobial activity against selected spoilage microorganisms. No antimicrobial effects were recorded with active zein and poly(ε-caprolactone). The water content of the polymeric matrix was the key parameter associated with antimicrobial effectiveness of this active system intended for food packaging applications.

In recent years, the interest in antimicrobial food packaging has increased considerably because of the potential use of an active system for prolonging the shelf life of packaged foods. Antimicrobial compounds can be either organic or inorganic *(6)*. Among inorganic compounds, silver nanoparticles (AgNPs), which have antibacterial properties, have been widely used in many fields including biomedical, food packaging, and water treatment applications. The antibacterial mechanism of silver is mainly related to the action of silver ions and metallic AgNPs. Silver ions have strong inhibitory and bactericidal effects *(36)*. These ions are highly reactive, bind to tissue proteins, and cause structural changes in the bacterial cell wall and nuclear membrane, leading to cell distortion and death. The mechanism of action of metallic silver is related to its interaction with sulfur-containing proteins found in the respiratory enzymes of bacterial cells. AgNPs bind to the bacterial cell wall and cell membrane and inhibit the respiration process *(18)* and cell division, leading to cell death *(12, 24, 30, 31)*.

Inorganic phyllosilicate clays have been used as support for AgNPs to generate a new class of antimicrobial systems. The platelet clays, which possess intensive charges on the surface, allow swelling in water and generate a stable pseudo-crosslinking network that interacts and stabilizes the AgNPs. Without organic surfactants, the Ag-clay complex exhibits high water stability *(11)*. The silver supporting material can control the release kinetics of silver ions because of weak electrostatic interactions, which are established with surface platelets of montmorillonite (MMT). Moreover, the use of clays can improve the barrier properties of polymers by creating a tortuous path for low-molecular-weight diffusing molecules *(5)*. This feature is very important for polymeric materials to be used in food packaging applications.

Various methods have been reported for dealing with the preparation of AgNPs. Mainly the process consists of two steps: reduction of silver cations mostly from $AgNO_3$ solutions and stabilization of the resulting AgNPs. There are several methods for Ag^+ reduction, such as the use of reducing agents (generally sodium borohydride) *(1, 11, 22, 25, 32, 35),* gamma irradiation *(37),* UV irradiation *(8, 15),* and heating of an $AgNO_3$ solution *(33)*. Studies of the antimicrobial activity of the obtained nanoparticles revealed growth inhibition of various pathogens, including *Staphylococcus aureus, Pseudomonas aeruginosa, Streptococcus pyrogenes,* and methicillin- and oxycillin-resistant *S. aureus (32), Escherichia coli,* and *Enterococcus faecium (22, 37).*

When using silver in food packaging applications, the antimicrobial effectiveness of polymeric nanocomposites strongly depends on the hydrophilic nature of the polymeric matrix and on boundary conditions, such as pH and the ionic strength of the release solution *(19)*. Furthermore, the use of silver in highly filled systems is a viable approach for avoiding direct contact with food. This aspect is particularly important to satisfy the European Union safety regulations regarding the presence of silver ions in food matrices, which

* Author for correspondence. Tel: (+39) 881 589 242; Fax: (+39) 881 589 242; E-mail: ma.delnobile@unifg.it.

is limited to 0.05 mg/kg, a level not biocidal in food *(13)*. An et al. *(2)* investigated the application of AgNPs-polyvinylpyrrolidone as a coating for green asparagus and found that the antimicrobial coating increased the shelf life of asparagus by about 10 days at 2°C. Fernandez et al. *(13)* used a cellulose-based absorbent pad as a holder for AgNPs formed in situ by physical and chemical reduction methods. The hybrid materials developed by physical methods (UV and heat) were effective against pathogenic microorganisms in vitro, and positive results were obtained in assays with chicken exudates, both for mesophilic and lactic acid bacteria. The antimicrobial activity of the obtained material was mostly related to the released Ag^+ ions. These results suggested that the release of the bound silver from cellulose might be triggered after hydration.

The objectives of the present work were (i) to obtain Ag-MMT nanoparticles by allowing silver ions from silver nitrate ($AgNO_3$) to replace the exchangeable Na^+ counter ions in the natural sodium MMT, (ii) to develop active packaging systems embedding the Ag-MMT nanoparticles into different polymer matrices, and (iii) to investigate the dependence of Ag-MMT antimicrobial activity on the nature of the polymer. In particular, the Ag-MMT nanoparticles were chemically characterized and embedded into three polymer matrices: agar, zein, and poly(ε-caprolactone) (PCL). In vitro tests were performed to evaluate the antimicrobial effects of the nanocomposites against three strains of *Pseudomonas* spp. isolated from spoiled mozzarella cheese. The influence of both Ag-MMT content and of the water uptake of the polymer was investigated in relation to the antimicrobial effect.

MATERIALS AND METHODS

Reagents and polymers. The unmodified pristine clay (Na^+-MMT) was purchased from Southern Clay Products, Inc. (Gonzales, TX). Zein, ethanol, glycerol, and $AgNO_3$ were purchased from Sigma-Aldrich (Milan, Italy). Agar was purchased from Oxoid (Milan, Italy), and commercial grade PCL (CAPA 6501) was supplied by Solvay (Warrington, UK) in the form of granules.

Preparation of Ag-MMT nanoparticles. The Ag-MMT nanoparticles were prepared by ion exchange reaction. Five grams of Na-MMT was dispersed in 100 ml of a 0.2 M NaCl solution for 4 h while stirring. The solid was then separated by centrifugation (model 4239R, ACL International, Milan, Italy) at 10,000 rpm for about 15 min and then washed three times with deionized water. The washed Na-MMT was brought in contact with $AgNO_3$ solutions at various concentrations. Na-MMT was dispersed first in a 500-ppm $AgNO_3$ solution at 70°C for 3 h while stirring. The top and side of the beaker were covered to prevent exposure to UV room light. The solid and liquid parts of the slurry were separated by centrifugation at 10,000 rpm for 15 min. The collected solid part was brought into contact with 1,000- and 5,000-ppm $AgNO_3$ solutions following the procedure previously described. The final collected sediment was washed three times with deionized water and then allowed to dry overnight in a vacuum oven at 80°C. Dried samples were ground until a homogeneous powder was obtained.

Ag-MMT nanocomposite preparation. Zein solution was obtained by dissolving 5 g of zein (38 kDa) into 16 ml of 96% ethanol at 50°C. One gram of glycerol was added, and the solution was stirred with a magnetic stirring device (RCT basic, IKA Labortechnik, Staufen, Germany) for 10 min. The agar-water mixture was obtained by dissolving agar (8 g/liter; Oxoid) into distilled water at 121°C for 15 min. Ten grams of PCL was placed in a graduated tube and dissolved in 100 ml of dichloromethane with a mechanical stirrer. After cooling to room temperature, aliquots (5 ml) of zein solution, agar solution, and PCL solution were mixed with 10, 15, and 20 mg, respectively, of Ag-MMT. Each active solutions was put in a sonication bath for 5 min, placed in a tube, and cooled at ambient temperature under a laminar flow hood (Asalair, Milan, Italy) until the solvent was completely evaporated (about 24 h). All nanocomposites were completely transparent. As controls, zein, agar, and PCL solutions without nanoparticles also were prepared.

Ag-MMT and Ag-MMT nanocomposite characterization. Ag-MMT has been chemical characterized through the determination of silver content and UV-visible observation tests. The silver content of the modified MMT was determined by inductively coupled plasma mass spectrometry (ICP-MS) after dissolution of the MMT samples in hydrofluoric acid and nitric acid.

UV-visible absorption spectra were measured with a Lambda 850 spectrometer (Perkin Elmer, Foster City, CA). All spectra were recorded using quartz cuvettes within the range of 200 to 800 nm. The cuvettes were filled with a 500-ppm shaken water dispersion of Na-MMT and Ag-MMT, and their spectra were recorded. The Ag spectrum was isolated by subtracting the Na-MMT spectrum from the Ag-MMT spectrum.

The structures of Na-MMT and Ag-MMT clays and of Ag-MMT nanocomposite films were evaluated using wide angle X-ray diffraction (WAXD) measurements. An SAXSess diffractometer (40 kV, 50 mA; Anton Paar, GmbH, Graz, Austria) equipped with a Cu-Kα radiation source ($\alpha = 0.1546$ nm) and an image plate detector was used. The spectra were collected in the transmission mode (i.e., the X-ray beam moves through the sample) by scanning the 2θ (θ is the diffraction peak angle) range between 1.5 and 40°. All spectra were corrected only for the dark current and the empty holder background.

Microbial cocktail preparation. To determine the antimicrobial effects of AgNPs incorporated into the three polymeric matrices, growth experiments were carried out. Three strains of *Pseudomonas* isolated from spoiled mozzarella cheese were used for testing. Plate count broth (PCB; Oxoid) (5 g/liter tryptone, 1 g/liter glucose, and 2.5 g/liter yeast extract) was used as the culture medium *(9)*. All *Pseudomonas* strains were maintained on slants of appropriate medium and stored at 4°C as stock cultures. Before use, exponentially growing cultures were grown overnight in the appropriate liquid medium at the optimal temperature. After 24 h, a cocktail of the three strains was prepared by mixing 1% of each culture. Inocula were prepared by diluting the exponentially growing cultures with sterile saline solution (9 g/liter NaCl) to obtain approximately 10^3 CFU/ml. To ensure a high reproducibility in the inoculum preparation procedure, cell counts were standardized through the direct plate count technique.

In vitro evaluation of silver nanocomposite effectiveness. For the growth experiments, PCB was spread in the tubes containing the various active and control films. All tubes were inoculated with 70 ml of the prepared microbial cocktail (1%) and incubated at 25°C for 70 h. Periodically (at 0, 5, 23, 26, 29, 46, 53, and 70 h), 1-ml aliquots were taken from each tube for microbiological analyses. To avoid modification of the microbial concentration due to sampling, each tube was used for only a single measure. Each sample was decimally diluted serially with sterile

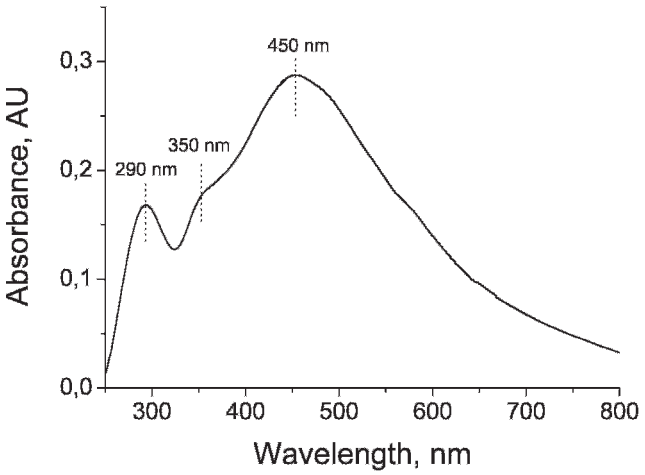

FIGURE 1. *UV-visible absorption spectra of silver Na-MMT.*

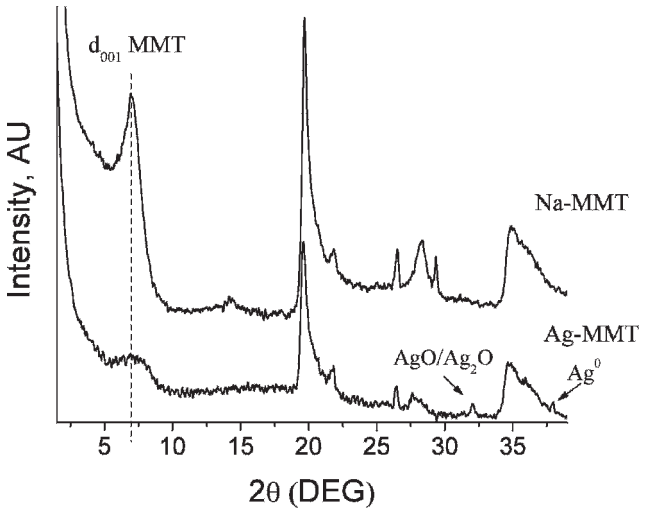

FIGURE 2. *XRD spectra of Na-MMT and Ag-MMT clays.*

saline solution (9 g/liter NaCl). Serial dilutions of samples were plated on *Pseudomonas* agar base modified by adding *Pseudomonas* cephaloridine-fucidin-cetrimide selective supplement after autoclaving at 121°C for 15 min, and plates were incubated at 25°C for 48 h. As controls, tubes of inoculated PCB without film also were monitored. All analyses were performed twice.

Modeling of microbial data. To quantitatively compare the microbial effectiveness of the active packaging systems, the Gompertz equation, as reparameterized by Zwietering et al. *(38),* was fitted to the experimental data:

$$\log N(t) = \log N_0 - A\cdot\exp\left\{-\exp\left\{\left[(\mu_{max}\cdot 2.71)\cdot\frac{\tau}{A}\right]+1\right\}\right\} + A\cdot\exp\left\{-\exp\left\{\left[(\mu_{max}\cdot 2.71)\cdot\frac{\tau - t}{A}\right]+1\right\}\right\} \quad (1)$$

where $N(t)$ is the viable cell concentration at time t, N_0 is the initial cell concentration, A is related to the difference between the decimal logarithm of the initial cell concentration and the decimal logarithm of the bacterial growth attained at the stationary phase, μ_{max} is the maximal specific growth rate, and τ is the lag time.

Water uptake. To study film hydration, the weight of the dry polymer and the weight of the film soaked for 70 h in the microbial broth at 25°C were measured. These conditions were chosen to simulate previous microbial growth experiments. The increase in water uptake (*%M*) was determined according to the expression:

$$\%M = \frac{W_f - W_i}{W_i}\cdot 100 \quad (2)$$

where W_f is the film weight after 70 h of hydration and W_i is the weight of the dry polymer contained in each film. The weight was assessed with a digital precision balance (Gibertini, Milan, Italy). All analyses were performed five times, and the mean of all measures was calculated.

Statistical analyses. To determine whether significant differences ($P < 0.05$) existed among the mean values of the fitting parameters, a one-way analysis of variance and Duncan's multiple range test with the option of homogeneous groups were used (STATISTICA 7.1 for Windows, StatSoft, Inc., Tulsa, OK).

RESULTS AND DISCUSSION

Ag-MMT chemical characterization. To obtain Ag-MMT nanoparticles, $AgNO_3$ was added to a water dispersion of MMT clays and heated to promote both the ionic exchange with sodium ions and silver reduction. After addition of $AgNO_3$, an immediate color change was observed due to the formation of an Ag^+-clay complex *(34).* During heating at 70°C, partial reduction of Ag^+ to Ag^0 occurred, and the color of the dispersion changed to deep violet.

The silver content of the Ag-MMT clays was determined by ICP-MS analysis after dissolution in a mixture of hydrofluoric acid and nitric acid. The Ag concentration was 0.037 g/g, which is comparable to the maximum concentration of Ag^+ absorbed on MMT that was obtained by Praus et al. *(26).*

The UV-visible absorption spectrum related to silver is shown in Figure 1. Characteristic silver surface plasmon bands were detected at 290, 350, and 450 nm, and these bands were tentatively ascribed to the presence of residual silver ions *(35)* or with the existence of silver nanoparticles smaller than 2 nm *(28),* smaller than 10 nm *(15),* and smaller than 40 nm *(29),* respectively. The broad peak at 450 nm is indicative of the presence of silver nanoparticle aggregates.

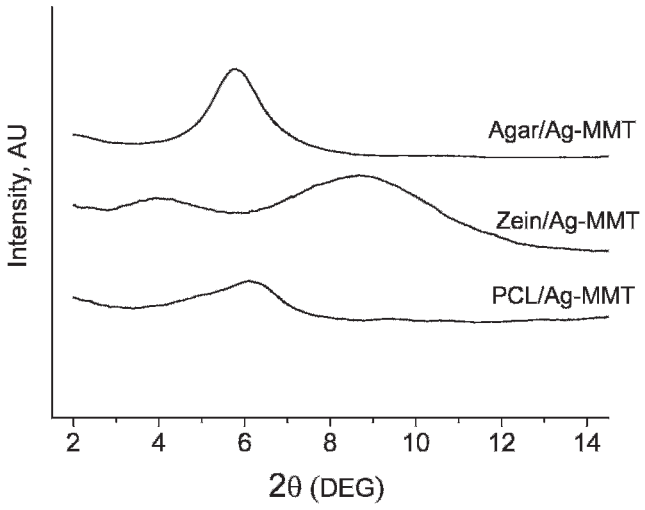

FIGURE 3. *XRD spectra of the agar, zein, and PCL nanocomposites.*

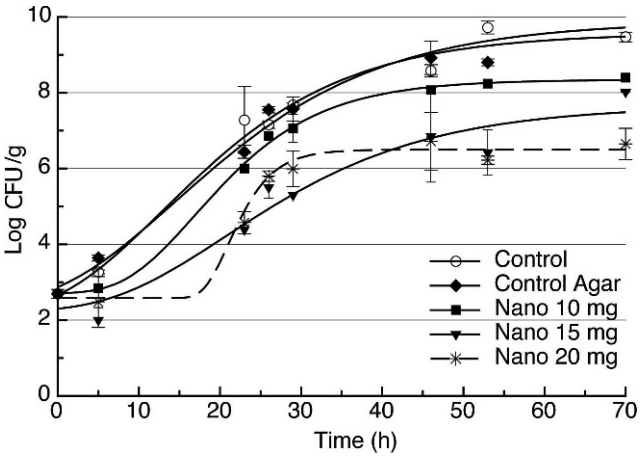

FIGURE 4. *Changes in* Pseudomonas *spp. viable cells plotted as a function of storage time for all tested samples of agar-based nanocomposites.*

X-ray diffraction analyses of Ag-MMT and Ag-MMT nanocomposites. X-ray diffraction (XRD) analyses of Na-MMT and Ag-MMT clays were conducted to highlight the MMT structural modifications that take place when Ag ions replace Na ions (along with K, Mg, and Ca ions) and silver nanoparticles locate onto the MMT layered structure. Using this approach, it is possible to roughly estimate the location of the silver within the MMT structure (i.e., in the galleries or on the surface of MMT platelets).

The XRD spectra of Na-MMT and Ag-MMT powders are compared in Figure 2. Unmodified Na-MMT clay has an intense diffraction peak at around $2\theta = 7.2^\circ$, corresponding to a basal d_{001} spacing between the silicate platelets of about 1.2 nm. The MMT modified with Ag also had a distinctive diffraction peak at $2\theta = 7.2^\circ$, but the peak shape and intensity was markedly different from that of the Na-MMT clay. These features reflect the structural modifications that take place when Ag ions replace Na ions inside the layered structure of MMT. MMT clay probably loses its layered structure, giving rise to nanoparticles with collapsed or exfoliated structure *(26)*. The occurrence of structural modifications also was indicated by the disappearance of the Na-MMT peak at 2θ around 29°. An additional small peak with maximum at $2\theta = 37.9^\circ$ in the XRD pattern of Ag-MMT corresponds to the (111) reflection of Ag, thus proving the presence of metallic silver. The diffraction peak at 2θ around 32° can be assigned to AgO-Ag_2O crystalline domains, which are generated as a result of a limited reduction of Ag ions under basic conditions *(29)*.

The average size of the Ag crystalline nanodomains (L) can be estimated using Scherrer's formula, $L = 0.9\lambda/\beta \cos\theta$, where λ is the radiation wavelength (0.154 nm for CuKα), β is the width at half-height, and θ is the diffraction peak angle. The obtained average size is about 40 nm, which confirms the results of the UV analysis. Because the basal spacing d_{001} of MMT is around 1.2 nm and most MMT are in the collapsed or exfoliated structure, the metallic AgNPs and silver ions must be located on the surface of the MMT platelets.

The WAXD spectra for Ag-MMT nanocomposite films are shown in Figure 3. The diffraction peak associated with the basal d_{001} spacing between the silicate platelets is at 2θ around 6, 5.8, and 4° for PCL–Ag-MMT, agar–Ag-MMT, and zein–Ag-MMT nanocomposites, respectively. The diffraction peak at $2\theta = 8.5^\circ$ evident in the zein–Ag-MMT spectrum arises from the zein α-helix regularly packed in hexagonal domains *(23)*. The macromolecules of PCL, zein, and agar intercalate the silicate platelets to a different extent. Zein displays a higher capability to intercalate Ag-MMT, probably because of a better interaction with the hydrophilic internal surface of silicate platelets *(20)*.

Antimicrobial activity of Ag-MMT–based nanocomposite films. The effectiveness of AgNPs immobilized in zein, agar, and PCL was tested against three strains of *Pseudomonas* spp. The main reason for choosing these bacteria was that the *Pseudomonadaceae* are considered foodborne bacteria *(4),* in particular spoilage microorganisms of fresh dairy products *(7, 10, 14)*. The active system developed in this study also could be applied to a packaged product containing a brine, such as mozzarella cheese. The in vitro analyses were performed for 70 h to achieve clear microbial growth.

Figure 4 illustrates the changes in the *Pseudomonas* spp. counts, plotted as a function of the storage period, after contact with control samples and the agar-based nanocomposites. In the data related to both the control samples, the following trend was noted: a short lag phase was followed by a continuous increase in the viable cell concentration until the stationary phase was attained. The *Pseudomonas* population proliferated from 10^2 to 10^9 or 10^{10} CFU/g during the 70 h of monitoring. In contrast, the Ag-MMT nanoparticles embedded in agar were effective at inhibiting microbial growth. After 24 h of incubation, the *Pseudomonas* colonies were present in all the tubes regardless of the silver content, but the CFU decreased significantly as the silver content increased. The results from the fitting

TABLE 1. *Parameter values obtained by fitting equation 1 to the experimental data relative to agar-based nanocomposites*[a]

Sample	N_0 (log CFU/g)	μ_{max} (Δ log CFU/g/day)	τ (day)	A (log CFU/g)
Control	2.66 ± 0.27 A	0.21 ± 0.02 A		7.40 ± 0.4 B
Control agar	2.87 ± 0.32 A	0.19 ± 0.02 A		7.52 ± 0.5 B
Nano, 10 mg	2.71 ± 0.11 A	0.24 ± 0.03 A	8.32 ± 2.48 A	5.64 ± 0.18 A
Nano, 15 mg	2.30 ± 0.53 A	0.14 ± 0.07 A	6.52 ± 14.38 A	5.43 ± 1.53 A
Nano, 20 mg	2.58 ± 0.17 A	0.47 ± 0.14 A	18.69 ± 1.6 A	3.93 ± 0.22 C

[a] Values are mean ± standard deviation. Within the same column, means with different letters are significantly different.

TABLE 2. *Parameter values obtained by fitting equation 1 to the experimental data relative to zein-based nanocomposites*[a]

Sample	N_0 (log CFU/g)	μ_{max} (Δ log CFU/g/day)	τ (day)	A (log CFU/g)
Control	2.66 ± 0.27 A	0.21 ± 0.02 A		7.40 ± 0.4 A
Control zein	2.74 ± 0.48 A	0.19 ± 0.03 A		7.26 ± 0.72 A
Nano, 10 mg	2.45 ± 0.76 A	0.33 ± 0.18 A	0.05 ± 8.33 A	5.73 ± 2.12 A
Nano, 15 mg	2.65 ± 0.94 A	0.31 ± 0.16 A	3.54 ± 7.74 A	5.43 ± 1.34 A
Nano, 20 mg	3.02 ± 0.7 A	0.43 ± 0.42 A	16.98 ± 7.43 B	5.14 ± 0.91 A

[a] Values are mean ± standard deviation. Within the same column, means with different letters are significantly different.

procedure are reported in Table 1, along with the statistical analyses. The values for the two control samples were similar, whereas for the active samples significant differences were obtained in the lag phase (τ) and in the cell populations attained at the stationary phase (A). All three silver concentrations seem to prolong the lag phase; the best result was achieved with the highest concentration. *Pseudomonas* has shown resistance to most essential oils and to all known antimicrobials and antibiotics because of a very restrictive outer membrane barrier that is highly resistant to even synthetic drugs. The hydrophilic cell wall structure of gram-negative bacteria is constituted essentially of lipopolysaccharides that block the penetration of hydrophobic oils and prevent the accumulation of essential oils in the target cell membrane *(3)*. The negative charges of the lipopolysaccharides probably attract the weak positive charges of the silver ions or nanoparticles, thus allowing the silver-based antimicrobial particles to be effective.

A nonsignificant antimicrobial effect was obtained with zein films (data not shown). A similar increase in microbial growth was recorded for the control samples and for all the investigated Ag-MMT loaded films. This effect was ascribed to the fact that the release of silver ions is governed by water transport properties of the coating *(19)*. Therefore, coatings with scarce hydrophilic components have limited water affinity and consequently low silver release. This bio-based polymeric material is more hydrophobic than other proteins because of the presence of the apolar amino acids of proline and glutamine, which are the main constituents of zein. By the fitting procedure (equation 1), the same parameters were calculated for each nanocomposite system. Marked differences between samples were found in the τ values (Table 2). The silver-based nanocomposites seemed to prolong the lag phase, and the lag phase increased with increased concentration of the active compound in the polymeric matrix. However, the prolongation of the lag phase of pseudomonads was followed by an increase in cell numbers during the storage period, probably because of recovery of stressed cells, as reported by Johnston and Brown *(16)* and Richards and Cavill *(27)*. The use of silver nanocomposite could cause reversible damage to the outer membrane, inhibiting the ability of cells to form colonies on plates. Under conditions of prolonged stress, the cells could repair the damages to the membrane and reacquire the ability to grow *(3)*.

AgNPs immobilized in PCL film did not markedly affect the growth cycle of the selected microbial strains (data not shown). The differences between parameter values calculated by fitting the equation were small and nonsignificant (Table 3), probably because of the limited hydrophilic character of PCL *(21)*. These findings further support the hypothesis that the affinity for water influences the ability to achieve an ionic exchange with silver ions *(19)*. The magnitude of this effect also depends on the nature and quantity of the silver particles and their distribution within the coating matrix *(17)*.

To understand the differences in the effectiveness of Ag-MMT embedded in the three matrices, water uptake tests of agar hydrogel, zein film, and PCL film were conducted (Figure 5). Results are in accordance with the antimicrobial data recorded for the three polymeric coatings. The matrix containing the highest water content was the agar hydrogel, thus suggesting the highest level of macromolecular mobility for this polymeric network. The hydrogel allowed the active species generated by AgNPs (i.e., Ag^+ or small AgNPs able to bind the bacterial cell wall) to diffuse more rapidly toward the bacteria than was possible in the hydrated zein and PCL films. The higher amount of water absorbed by the agar hydrogel enhanced the mobility of the active silver species.

Nanoparticles can be successfully used to prepare antimicrobial systems intended for food packaging applications. Ag-MMT antimicrobial nanoparticles can be easily prepared by replacing exchangeable Na^+ counter ions in the natural sodium MMT with Ag^+ ions and reducing these combinations to Ag metallic nanoparticles by thermal

TABLE 3. *Parameter values obtained by fitting equation 1 to the experimental data relative to PCL-based nanocomposites*[a]

Sample	N_0 (log CFU/g)	μ_{max} (Δ log CFU/g/day)	τ (day)	A (log CFU/g)
Control	3.77 ± 0.46 A	0.27 ± 0.04 A	0.07 ± 6.50 B	6.56 ± 1.35 A
Control PCL	4.06 ± 0.25 A	0.35 ± 0.08 A	7.63 ± 4.42 A	5.89 ± 0.31 A
Nano, 10 mg	4.06 ± 0.04 A	0.2 ± 0.008 A	6.83 ± 0.95 A	5.65 ± 0.11 A
Nano, 15 mg	4.00 ± 0.33 A	0.25 ± 0.07 A	7.27 ± 5.95 A	5.59 ± 0.49 A
Nano, 20 mg	3.97 ± 0.43 A	0.2 ± 0.05 A	4.76 ± 8.66 A	5.93 ± 0.96 A

[a] Values are mean ± standard deviation. Within the same column, means with different letters are significantly different.

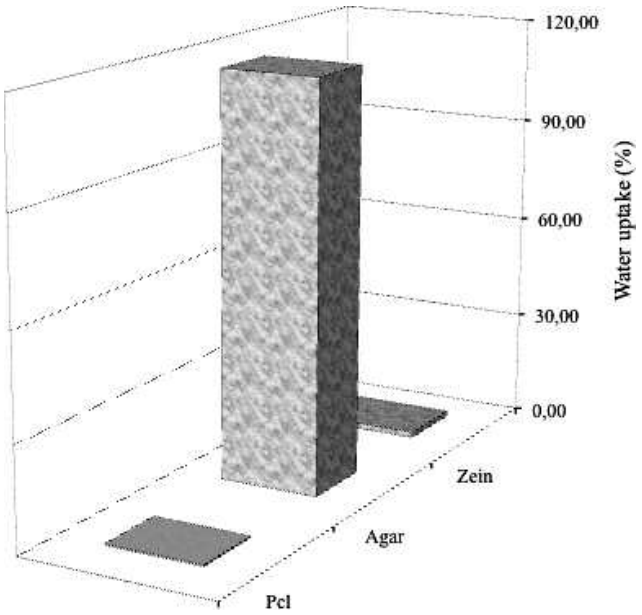

FIGURE 5. *Water uptake of agar, zein, and PCL nanocomposites.*

treatment. XRD analysis revealed that the MMT clays lose their layered structure, giving rise to collapsed or exfoliated structures, and that silver ions and nanoparticles are mainly located on the silicate platelets. UV-visible absorption spectrum analysis confirmed that both Ag^+ and Ag^0 nanoparticles can be found in the obtained Ag-MMT powder and that nanoparticle sizes range from a few to 40 nm. Water uptake by the organic matrix plays a key role in the antimicrobial efficacy. Because agar hydrogel had the highest water content, agar-based nanocomposites were the most active against the test microorganisms.

REFERENCES

1. Ahmad, Z., R. Pandey, S. Sharma, and G. K. Khuller. 2005. Alginate nanoparticles as antituberculosis drug carriers: formulation development, pharmacokinetics and therapeutic potential. *Indian J. Chest Dis. Allied Sci.* 48:171–176.
2. An, J., M. Zhang, S. Wang, and J. Tang. 2008. Physical, chemical and microbiological changes in stored green asparagus spears as affected by coating of silver nanoparticles–PVP. *LWT* 41:1100–1107.
3. Bezić, N., M. Skočibušić, V. Dunkić, and A. Radonić. 2003. Composition and antimicrobial activity of *Achillea clavennae* L. essential oil. *Phytother. Res.* 17:1037–1040.
4. Bishop, J. R., and C. H. White. 1986. Assessment of dairy product quality and potential shelf life—a review. *J. Food Prot.* 49:739–753.
5. Choudalakis, G., and A. D. Gotsis. 2009. Permeability of polymer/clay nanocomposites: a review. *Eur. Polym. J.* 45:967–984.
6. Conte, A., G. G. Buonocore, M. Sinigaglia, L. C. Lopez, P. Favia, R. d'Agostino, and M. A. Del Nobile. 2008. Antimicrobial activity of immobilized lysozyme on plasma-treated polyethylene films. *J. Food Prot.* 71:119–125.
7. Conte, A., C. Scrocco, M. Sinigaglia, and M. A. Del Nobile. 2007. Innovative active packaging systems to prolong the shelf life of mozzarella cheese. *J. Dairy Sci.* 90:2126–2131.
8. Darroudi, M., M. B. Ahmad, K. Shameli, A. H. Abdullah, and N. A. Ibrahim. 2009. Synthesis and characterization of UV-irradiated silver/montmorillonite nanocomposites. *Solid State Sci.* 11:1621–1624.
9. Del Nobile, M. A., A. Conte, A. L. Incoronato, and O. Panza. 2008. Antimicrobial efficacy and release kinetics of thymol from zein films. *J. Food Eng.* 89:57–63.
10. Del Nobile, M. A., D. Gammariello, A. Conte, and M. Attanasio. 2009. A combination of chitosan, coating and modified atmosphere packaging for prolonging Fior di latte cheese shelf life. *Carbohydr. Polym.* 78:151–156.
11. Dong, R. X., C. C. Chou, and J. J. Lin. 2009. Synthesis of immobilized silver nanoparticles on ionic silicate clay and observed low-temperature melting. *J. Mater. Chem.* 19:2184–2188.
12. Feng, Q. L., J. Wu, G. Q. Chen, F. Z. Cui, T. N. Kim, and J. O. Kim. 2000. A mechanistic study of the antibacterial effect of silver ions on *Escherichia coli* and *Staphylococcus aureus*. *J. Biomed. Mater.* 52: 662–668.
13. Fernández, A., E. Soriano, G. Lopez-Carballo, P. Picouet, E. Lloret, R. Gavara, and P. Hernandez-Muñoz. 2009. Preservation of aseptic conditions in absorbent pads by using silver nanotechnology. *Food Res. Int.* 42:1105–1112.
14. Gammariello, D., S. Di Giulio, A. Conte, and M. A. Del Nobile. 2008. Effects of natural compounds of microbial safety and sensory quality of Fior di latte cheese, a typical Italian cheese. *J. Dairy Sci.* 91:4138–4146.
15. Huang, H., and Y. Yang. 2008. Preparation of silver nanoparticles in inorganic clay suspensions. *Comp. Sci. Technol.* 68:2948–2953.
16. Johnston, M. D., and M. H. Brown. 2002. An investigation into the changed physiological state of *Vibrio* bacteria as a survival mechanism in response to cold temperatures and studies on their sensitivity to heating and freezing. *J. Appl. Microbiol.* 92:1066–1077.
17. Kelly, P. J., H. Li, K. A. Whitehead, J. Verran, R. D. Arnell, and I. Iordanova. 2009. A study of the antimicrobial and tribological properties of TiN/Ag nanocomposite coatings. *Surf. Coat. Technol.* 204:1137–1140.
18. Klasen, H. J. 2000. A historical review of the use of silver in the treatment of burns. Part I. Early uses. *Burns* 30:1–9.
19. Kumar, R., and H. Münstedt. 2005. Polyamide/silver antimicrobials: effect of crystallinity on the silver ion release. *Polym. Int.* 54:1180–1186.
20. Luecha, J., N. Sozer, and J. L. Kokini. 2010. Synthesis and properties of corn zein/montmorillonite nanocomposite films. *J. Mater. Sci.* 45: 3529–3537.
21. Lyons, J. G., P. Blackie, and C. L. Higginbotham. 2008. The significance of variation in extrusion speeds and temperatures on a PEO/PCL blend based matrix for oral drug delivery. *Int. J. Pharm.* 351:201–208.
22. Malachova, K., P. Praus, Z. Pavlickova, and M. Turicova. 2009. Activity of antibacterial compounds immobilised on montmorillonite. *Appl. Clay Sci.* 43:364–368.
23. Matsushima, N., G. Danno, H. Takezawa, and Y. Izumi. 1997. Three-dimensional structure of maize α-zein proteins studied by small-angle X-ray scattering, *Biochim. Biophys. Acta* 1339:14–22.
24. Morones, J. R., J. L. Elechiguerra, A. Camacho, and J. T. Ramirez. 2005. The bactericidal effect of silver nanoparticles. *Nanotechnology* 16:2346–2353.
25. Praus, P., M. Turicova, and M. Klementova. 2009. Preparation of silver-montmorillonite nanocomposites by reduction with formaldehyde and borohydride. *J. Braz. Chem. Soc.* 20:1351–1357.
26. Praus, P., M. Turicova, and M. Valaskova. 2008. Study of silver adsorption on montmorillonite. *J. Braz. Chem. Soc.* 19:549–556.
27. Richards, R. M. E., and R. H. Cavill. 1976. Electron microscope study of the effect of benzalkonium chloride and edetate disodium on cell envelope of *Pseudomonas aeruginosa*. *J. Pharm. Sci.* 65:76–80.
28. Shao, K., and J. Yao. 2006. Preparation of silver nanoparticles via a non-template method. *Mater. Lett.* 60:3826–3829.
29. Sharma, V. K., R. A. Yngard, and Y. Lin. 2009. Silver nanoparticles: green synthesis and their antimicrobial activities. *Adv. Colloid Interface Sci.* 145:83–96.
30. Sondi, I., and B. Salopek-Sondi. 2004. Silver nanoparticles as antimicrobial agent: a case study on *E. coli* as a model for gram-negative bacteria. *J. Colloid Interface Sci.* 275:177–182.
31. Song, H. Y., K. K. Ko, L. H. Oh, and B. T. Lee. 2006. Fabrication of silver nanoparticles and their antimicrobial mechanisms. *Eur. Cells Mater.* 11:58.
32. Su, H. L., C. C. Chou, D. J. Hung, S. H. Lin, I. C. Pao, J. H. Lin, F. L. Huang, R. X. Dong, and J. J. Lin. 2009. The disruption of bacterial

membrane integrity through ROS generation induced by nanohybrids of silver and clay. *Biomaterials* 30:5979–5987.
33. Sun, X., and Y. Luo. 2005. Preparation and size control of silver nanoparticles by a thermal method. *Mater. Lett.* 59:3847–3850.
34. Top, A., and S. Ulku. 2004. Silver, zinc, and copper exchange in a Na-clinoptilolite and resulting effect on antibacterial activity. *Appl. Clay Sci.* 27:13–19.
35. Wang, H., X. Qiao, J. Chen, and S. Ding. 2005. Preparation of silver nanoparticles by chemical reduction method. *Colloids Surf. A Physicochem. Eng. Aspects* 256:111–115.
36. Yang, F. C., K. H. Wu, M. J. Liu, W. P. Lin, and M. K. Hu. 2009. Evaluation of the antibacterial efficacy of bamboo charcoal/silver biological protective material. *Mater. Chem. Physics* 113: 474–479.
37. Yoksan, R., and S. Chirachanchai. 2009. Silver nanoparticles dispersing in chitosan solution: preparation by γ-ray irradiation and their antimicrobial activities. *Mater. Chem. Physics* 115:296–302.
38. Zwietering, M. H., F. M. Jongenburger, M. Roumbouts, and K. Van't Riet. 1990. Modeling of the bacterial growth curve. *Appl. Environ. Microbiol.* 56:1875–1881.